Computer renormalization-group calculations of $2k_F$ and $4k_F$ correlation functions of the one-dimensional Hubbard model

J. W. Bray
General Electric Corporate Research and Development, Schenectady, New York 12301

S. T. Chui
Department of Physics, State University of New York at Albany, Albany, New York 12222
(Received 20 December 1978)

We calculate $2k_F$ and $4k_F$ charge-density wave (CDW) and spin-density wave (SDW) autocorrelation functions for the one-dimensional Hubbard model using a computer renormalization-group technique previously developed by us. We describe the method and expected accuracy of the results. The correlation functions are calculated for Hubbard parameter $U/t = 2,10,50$ and for two different band fillings. We obtain, describe, and compare for the first time the magnitudes and temperature dependences of the correlation functions. We find, *inter alia*, that the $4k_F$ instability arises at very large U and that the $2k_F$ SDW and $4k_F$ CDW dominate at large U.

I. INTRODUCTION

In an earlier paper (Ref. 1, hereafter designated I), we described a computer renormalization-group technique which we applied to the Hubbard model.[2] In this paper we use this technique to evaluate retarded density-density correlation functions at wave vectors $2k_F$ and $4k_F$, where k_F is the Fermi wave vector, all within the Hubbard model. Such calculations are important because real quasi-one-dimensional conductors, which have been the subject of feverish activity in recent years, usually show an instability at $2k_F$, which has been associated with the Peierls "transition."[3] They occasionally also show[4] an instability at $4k_F$, which has been demonstrated to occur in one-dimensional systems when the electron-electron Coulomb repulsion is large enough.[5-7] The Hubbard model is the simplest model of a one-dimensional system which contains important physics, viz., the on-site electron-electron Coulomb interaction U. Therefore, if we are to understand thoroughly the $2k_F$ and $4k_F$ instabilities, it is certainly important to understand them quantitatively in this model.

In Sec. II, we describe our computer renormalization-group technique and discuss the nature and accuracy of the results which may be expected from it. In Sec. III, we describe the calculation of the correlation functions and their expected accuracy. In Sec. IV, we present our results and discuss our observations and conclusions based on the relative magnitudes and temperature dependences of the correlation functions.

II. NUMERICAL TECHNIQUE

Our basic numerical technique is also described in I. The technique calculates the eigenfunctions and eigenvalues for chains for finite length Nd, where N is the number of sites and d is the uniform intersite spacing. The Hamiltonian solved for a chain with N sites is

$$H_N = \sum_{\substack{i=1 \\ \sigma}}^{N} (t a_{i\sigma}^{\dagger} a_{i+1,\sigma} + \text{H.c.}) + \sum_{i=1}^{N} U n_{i\uparrow} n_{i\downarrow}, \qquad n_{i\sigma} \equiv a_{i\sigma}^{\dagger} a_{i\sigma} \tag{1}$$

Here $a_{i\sigma}^{\dagger}$ ($a_{i\sigma}$) is the creation (destruction) operator for an electron on site i with spin σ, t is the nearest-neighbor transfer energy, and U is the on-site Coulomb repulsion. The model has two parameters: the ratio U/t and the average number of electrons per site, ρ.

In our iterative procedure (see I), the chain length is doubled at each stage of iteration, beginning with $N=2$. We have carried out this procedure for $N=2,4,8,16$. To facilitate computation, we group the eigenstates into manifolds characterized by charge, spin, and parity, all of which are good quantum numbers. We retained the 30 such charge-spin-parity manifolds which are closest in energy to the ground state. We diagonalized $L2$ states in each manifold: The $L1$ lowest in energy (relative to the ground state) we diagonalized by a standard matrix method and the rest by second-order perturbation theory. The $L3$ lowest-energy diagonalized states were retained. The rest must be discarded for $N \geq 6$ because there are simply too many to handle. As a result, controlled errors appear in the eigeninformation as N increases.

The best way to study these errors is to compare calculations having different numbers of retained states with exact results for a known case. This is done in Table I for the noninteracting half-filled band. As expected, the more states one retains,

TABLE I. Comparison of exact energies E_i of the first four excited states (relative to the ground state) with our numerical results for model parameters $U=0$, $\rho=1$, $N=16$. $L2$ is the number of states diagonalized in each charge-spin-parity manifold, and ($L2$–$L1$) of these are diagonalized by second-order perturbation theory. The $L3$ lowest-energy states are retained in each manifold after diagonalization.

$L1$	$L2$	$L3$	$8E_1/t$	$8E_2/t$	$8E_3/t$	$8E_4/5$
100	400	20	1.65	3.17	4.62	6.13
150	300	20	1.63	3.15	4.67	6.10
150	400	20	1.61	3.13	4.61	6.05
150	400	28	1.64	3.11	4.65	6.08
150	500	20	1.60	3.11	4.61	6.04
150	600	20		3.12	4.56	6.02
200	400	20	1.62	3.12	4.67	6.03
Exact energies[a]			1.476	2.952	4.378	5.904

[a] C. A. Coulson, Proc. R. Soc. A 164, 383 (1938); R. P. Messmer, Phys. Rev. B 15, 1811 (1977).

the smaller the errors. For the calculations presented in this paper, $L1=100$, $L2=200$, and $L3=24$, in the usual 30 manifolds, for a total of 6000 states retained per iteration. With these parameters, the maximum absolute eigenvalue error is less than $\sim 0.63N\%$ for $N \geq 8$ and ~ 0 for $N \leq 4$, since all states are retained. These error limits are obtained by comparison with exact calculations for $U=0$.

The reader should note that although the percentage error increases with each iteration, the magnitude of the calculated eigenvalues relative to the ground-state energy decreases as N^{-1} because the width in energy of the retained states decreases as N^{-1}. Therefore, the increased uncertainty of the eigenvalues is offset by their smaller values in such a way that they converge rather quickly toward the energy values for the infinite chain. This renormalization-group property is illustrated in Table II, where we have compared the calculated values of the ground-state energy E_0 for various finite chains with E_0 for the infinite chain, which is known exactly.[8] Note that the convergence for the two cases presented ($U/t=2, 10$) is good.

III. CALCULATION OF THE CORRELATION FUNCTIONS

The retarded density autocorrelation function for a chain with N sites is given by

$$D_N(k,\omega) = Z^{-1} \sum_{ij} (2\pi e^{-\beta E_i} |\langle i|n'(k)|j\rangle|^2 \times\{1-\exp[-\beta(E_j-E_i)]\} \times[\omega-(E_i-E_j)+i\eta]^{-1}) \quad (2)$$

where $Z=\mathrm{Tr}[\exp(-\beta H_N)]$, $n'(k)\equiv n(k)-\langle n(k)\rangle$, η is equivalent to the positive infinitesimal, and $\beta=T^{-1}$. For the charge-density calculation

$$n(k)=\sum_{\substack{j=1\\ \sigma}}^{N} e^{ikjd} a_{j\sigma}^{\dagger} a_{j\sigma}\,, \quad (3)$$

and for the spin density,

$$n(k)=\sum_{\substack{j=1\\ \sigma}}^{N} e^{ikjd}\sigma a_{j\sigma}^{\dagger} a_{j\sigma}\,. \quad (4)$$

In Eq. (2), i and j denote eigenstates, with $|j\rangle$ an eigenfunction and E_j an eigenvalue. We take the Boltzmann constant $k_B=1$.

The matrix elements $\langle i|n(k)|j\rangle$ are computed

TABLE II. Comparison of the ground-state energy E_0 calculated by our method for finite chains with the exact results for the corresponding infinite chain. N_e is the number of electrons in a chain with N sites.

	N	N_e	$-E_0/tN$ (calculated)	$-E_0/tN$ (infinite chain[a])	% difference
$\rho=1$, $U/t=2$	2	2	0.618		26
	4	4	0.719	0.84	14
	8	8	0.778	for all N	7
	16	16	0.805		4
$\rho=\pi^{-1}$, $U/t=2$	2	1	0.500	0.71	30
	4	1	0.405	0.48	16
	8	3	0.614	0.66	7
	16	5	0.549	0.57	4
	32	10	0.553	0.57	3
$\rho=\pi^{-1}$, $U/t=10$	2	1	0.500	0.68	26
	4	1	0.405	0.48	16
	8	3	0.571	0.62	8
	16	5	0.524	0.55	5

[a] H. Shiba, Phys. Rev. B 6, 930 (1972).

iteratively beginning with the eigenfunctions for the two-atom chain. Computation is facilitated by dealing exclusively with reduced matrix elements and their appropriate 6-J symbols and then converting these to full matrix elements before using them to compute correlation functions. The coefficients produced by the diagonalization routines are used to relate the matrix elements for the $2N$-site chain to those for the N-site chain. The value of k determines the phase between the two N-site chains which combine to give the $2N$ chain. We normalize the matrix elements with a factor of $N^{-1/2}$.

We have computed both the real (Re) and imaginary (Im) parts of D_N as a function of temperature T at $k=2k_F, 4k_F$ and $\omega=0$. The Re part contains contributions to Eq. (2) when $E_i \neq E_j$. The Im part contains the contribution when $E_i = E_j$, which is imprecisely defined when $\omega=0$. We have chosen to calculate the Im part which appears in the scattering cross section:

$$\mathrm{Im}[D_N(k,0)] = Z^{-1} \sum_{E_i=E_j} [2\pi e^{-\beta E_i} |\langle i|n(k)|j\rangle|^2]. \quad (5)$$

Note that we have used n instead of n' here so that the Bragg scattering is included. Since E_i has the aforementioned errors for $N \geq 8$, we have taken $E_i = E_j$ whenever the stated error limits of E_i and E_j overlap. Note also that only the lowest-energy level of short chains will contribute to Eq. (5) at $T \simeq 0$. In an infinite chain, the energy levels form a continuum, and the number of contributing states is $N(E_F)$, the density of states at the Fermi surface. Renormalization-group calculations suggest that $N(E_F)$ is not strongly affected by infrared divergences.[9] We thus expect $N(E_F) \propto N$. Therefore, to compare properly numbers presented for the Im parts in Sec. IV to the infinite chain, one should multiply them by $N(E_F)$.

As discussed in I, the correlation functions are reasonably accurate only up to a certain temperature for $N \geq 8$ because of the elimination of the higher-lying states. The contributions of the higher-lying states fall off exponentially ($e^{-\beta E_i}$) in thermodynamic functions and the Im parts of the correlation functions, but the Re part connects the ground and low-lying states i with high-lying states j in a way that falls off only as $(E_j - E_i)^{-1}$. Consequently, the Im part has an absolute error[1] of less than $\sim 1.9N\%$ in the temperature range $T \leq 3.2t/N$ for $N \geq 8$ (error ~ 0 for $N \leq 4$). This is based on exact calculations for $U=0$. The error limits of the Re part cannot be so easily stated because the importance of the connected high-lying states varies with such factors as the presence of energy gaps. We found in I that the Re part is not much more than 50% accurate within the same temperature restrictions as the Im part, at least if a gap is present. The reader should note that we are discussing absolute errors here. Since these errors affect all the correlation functions similarly, conclusions based upon comparisons of several correlation functions should be much more accurate.

We have chosen to perform our main calculations at $\rho = \pi^{-1}$ because this is far from the half-filled band ($\rho = 1$) and is obviously incommensurate. Such a choice does introduce some extra details into the calculation. The finite chains computed at each stage must have a finite integer number of electrons. Therefore $\rho = \pi^{-1}$ must be approximated for each N by the most appropriate electron number N_e. These values are

N	N_e
2	1
4	1
8	3
16	5

(6)

For $N=16$, the actual site occupation (N_e/N) differs from π^{-1} by only 2%. Since $N_e = 1$ for $N = 2, 4$, the electron-electron correlation functions are not useful and are not presented for these N values in Sec. IV. The final detail is that $2k_F$ was computed with the formula $2k_F = \pi\rho/d$; i.e., the desired (limiting) electron site occupation was used. Calculations have also been performed with the definition $2k_F = \pi(N_e/N)/d$, and the results differ quantitatively somewhat but not qualitatively from those presented in Sec. IV.

IV. RESULTS AND DISCUSSIONS

Table III gives values of the charge-density (CDW) and spin-density (SDW) autocorrelation functions for $k = 2k_F$, $4k_F$ and $\omega = 0$. The values of the model parameters for which computations were made are $\rho = \pi^{-1}$ and $U/t = 2, 10, 50$. Since the table is for comparative purposes, it contains one datum point taken at $T = 0.05t$ to represent the low-temperature behavior of the Re and Im parts of each correlation function. Correlation functions for the half-filled band ($\rho = 1$) have also been computed at $U/t = 0, 2$ and were reported in I. However the half-filled band can be solved by much simpler means and is less interesting than partial band filling, which is the situation in the interesting real systems.

Among the new information gained through this study is the strength of the $2k_F$ and $4k_F$ instabilities

TABLE III. Values of real (Re) and imaginary (Im) parts of charge-density (CDW) and spin-density (SDW) autocorrelation functions $D_N(k, \omega=0)$ at $k=2k_F$, $4k_F$ and at temperature $T=0.05t$. The site occupation number $\rho=\pi^{-1}$. The number of sites is N.

		$D_N(2k_F,0)$				$D_N(4k_F,0)$			
		CDW		SDW		CDW		SDW	
		Re	Im	Re	Im	Re	Im	Re	Im
$U/t=2$	$N=8$	0.41	0.020	1.0	0.18	0.17	0.004	0.38	~0
	$N=16$	0.21	0.030	1.1	0.12	0.027	0.0002	0.019	0.0006
$U/t=10$	$N=8$	0.24	0.080	2.5	0.30	0.16	0.053	0.54	0.004
	$N=16$	0.035	0.069	1.8	0.16	0.11	0.012	0.047	0.002
$U/t=50$	$N=8$	0.20	0.11	3.1 10.1[a]	0.22 0.35[a]	0.22	0.088	0.59	0.024
	$N=16$	0.016	0.079	1.9 3.6[a]	0.089 0.18[a]	0.14	0.020	0.062	0.003

[a] Second number taken at $T=0.01t$, indicating rapid increase as $T\to 0$.

for various values of U/t. The excitation spectrum of the Hubbard model for arbitrary U and ρ has been calculated approximately by Coll.[10] However, the spectral weights, i.e., the strength of the various excitations, was not known before this work. Comparison of the numbers in Table III gives the information on relative strengths at low temperature. A number of observations and conclusions may be drawn.

(i) As noted before, the Im part of the correlation functions measures almost totally the ground-state character at low temperature because of the $e^{-E/T}$ factors. The Re part, on the other hand, connects the ground and excited states in a much less damped manner, and therefore it expresses excited-state character as well at low temperature. The Re part consequently has less absolute accuracy. The Im part also expresses the scattering factor, whereas the Re part is connected to coupling constants such as electron-phonon coupling. The point here is that the trends of the Re and Im parts may not always agree.

(ii) In basic agreement with other calculations,[5-7] we find that the $4k_F$ instability arises as a result of strong Coulomb repulsion ($U/t \gg 0$). At $U/t=2$, the instability is still much weaker than all others showed. As U increases, it grows steadily stronger.

(iii) At $4k_F$, the CDW instability is much larger than the SDW as judged by the Im part at $U/t=10, 50$. The Re part of the CDW is also larger at $N=16$. They are more comparable at $U/t=2$. Note that the Re SDW values drop very sharply from $N=8$ to 16. This indicates that finite-chain-size effects are present at $N=8$ and that the SDW is truly very small in the long chains. Therefore, we expect the $4k_F$ instability to be dominated by the CDW at large U.

(iv) At $2k_F$, the most obvious fact is the complete dominance of the SDW over both the CDW and all $4k_F$ instabilities for all calculated values of U/t. This dominance increases as U increases. The reader should note that the SDW and CDW are identical for $U=0$. Therefore, this dominance arises quickly as U increases. The SDW steadily increases as U increases and increases very rapidly as $T\to 0$ at large U. The $T=0.01t$ values of the SDW are included at $U/t=50$ to show this strong divergence.

(v) The $2k_F$ CDW, while much smaller than the SDW, is present for the U/t values calculated. As U increases, the Re part of the CDW decreases, and it decreases sharply from $N=8$ to 16 at $U/t=10, 50$, indicating it is very small in long chains. However, the imaginary part increases slightly with U and furthermore usually increases somewhat with temperature. Therefore, the Coll[10] picture that the $2k_F$ charge excitations disappear for large U does not appear to be completely correct except perhaps at much larger U than we consider. They are comparatively very weak, but present. Analytic calculations like those in Ref. 6 support this conclusion.

(vi) The $2k_F$ and $4k_F$ CDW make an interesting comparison. At $U/t=2$, the $2k_F$ CDW completely dominates. At $U/t=10$, the $2k_F$ CDW is still larger (except for the Re part, $N=16$), but comparable. At $U/t=50$, the Re part of the $4k_F$ CDW is larger but its Im part is still somewhat smaller. Therefore, it appears that these two instabilities are comparable for $U/t \geq 10$ at least up to ~50.

Valuable information may also be obtained from the temperature dependence of the correlation functions. Figs. 1 and 2 present a group of correlation functions versus temperature up to the maximum temperature at which they are valid ($T \lesssim 0.4t$ and $0.2t$ for $N=8$ and 16, respectively, as previously discussed). We chose to present the $4k_F$ CDW and $2k_F$ SDW because these are the stronger instabilities at each k value, and in tetrathiaful-

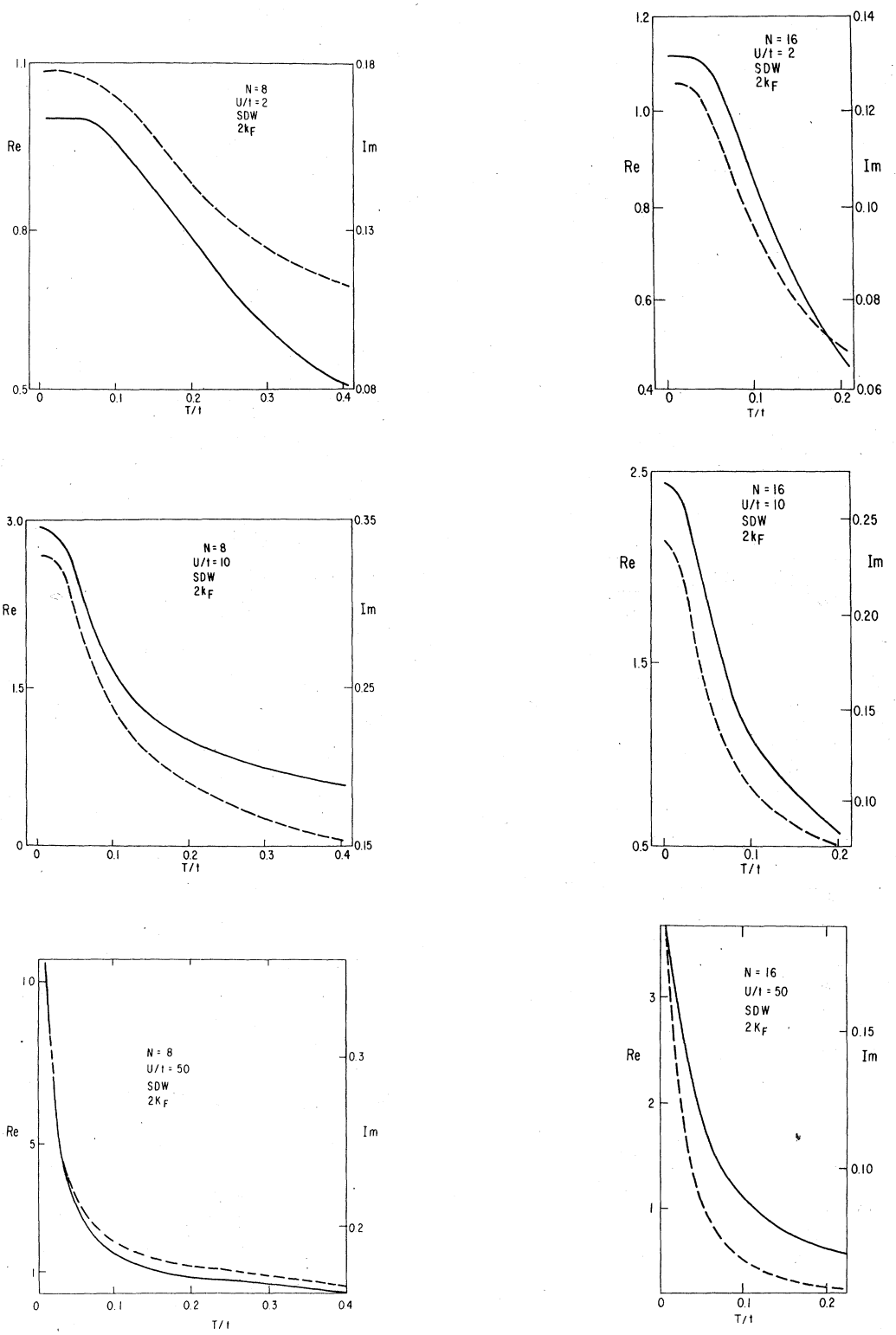

FIG. 1. (a)–(f) Spin-density (SDW) autocorrelation functions $D_N(k=2k_f, 0)$ for chains with number of sites $N=8$, 16. The left-hand-side axis is the real (Re) part, depicted by the solid curve. The dashed curve is the imaginary (Im) part, scaled on the right-hand-side axis.

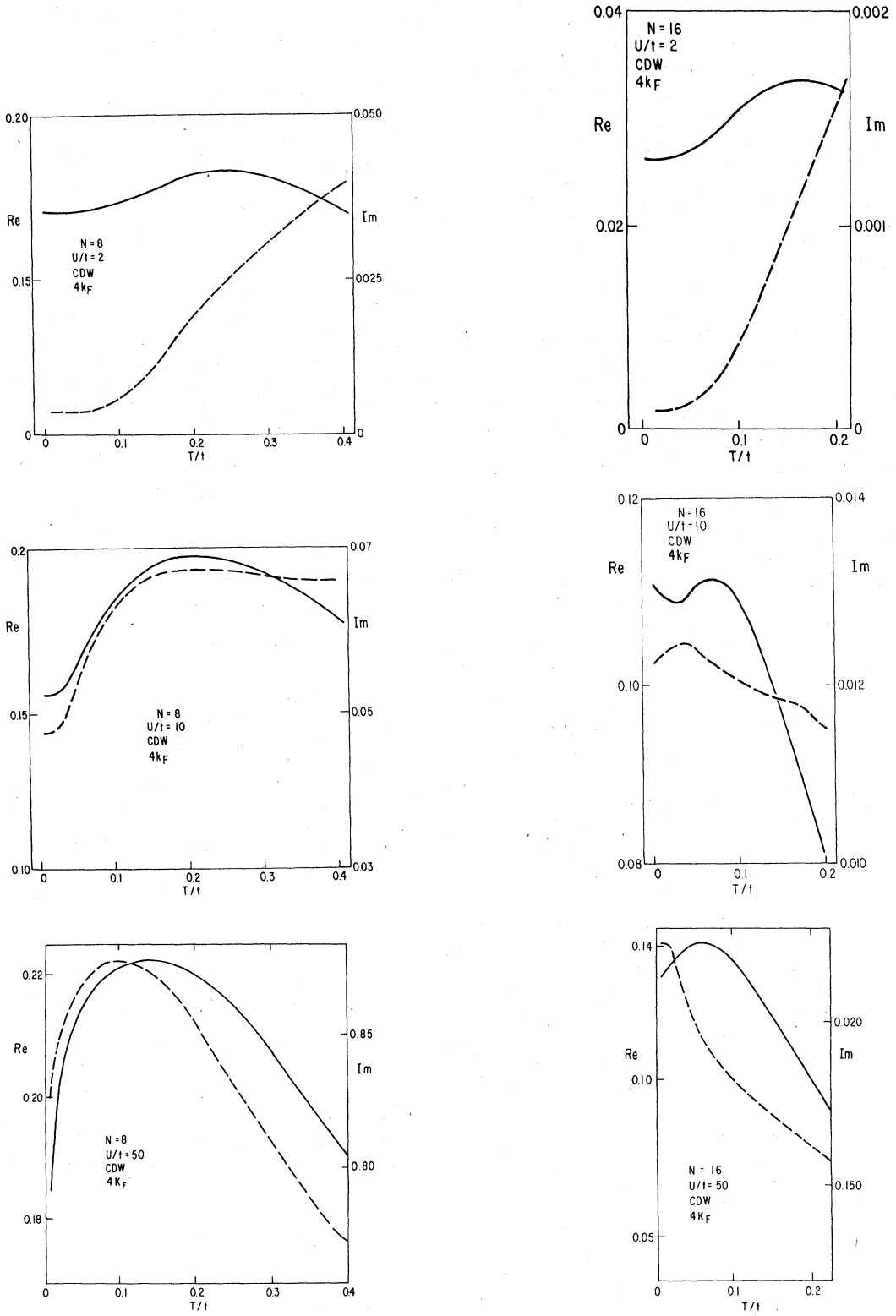

FIG. 2. (a)–(f) Charge-density (CDW) autocorrelation functions $D_N(k=4k_f, 0)$ for chains with number of sites $N=8$, 16. The left-hand-side axis is the real (Re) part, depicted by the solid curve. The dashed curve is the imaginary (Im) part, scaled on the right-hand-side axis.

valenium-tetracyanoquinodimethanide (TTF-TCNQ) the $4k_F$ and $2k_F$ instabilities have markedly different T dependences.[11] In this material, $4k_F$ dominates at room temperatures while $2k_F$ dominates a few tens of degrees above the transition at 54 K. Although the $4k_F$ CDW never dominates in the temperature range to which we are restricted, it does increase markedly relative to the $2k_F$ SDW. For instance, the ratios of SDW to CDW magnitudes decrease in the range depicted by a factor of 2–3 at $U/t=2$, by a factor of 3–6 at $U/t=10$, and by a factor of 2–3 (Im part) and 4–19 (Re part) at $U/t=50$.

Other observations of temperature dependences are limited only by what one is looking for. It is interesting to note that the $2k_F$ SDW decreases much more rapidly as a function of T at the large U values. Therefore, the $2k_F$ SDW increases much less drastically with U at $T \gg 0$. The existence of a peak at finite temperature in many of the $4k_F$ CDW functions indicates that it is the low-lying excited states which are strongest in $4k_F$ character, not the ground state.

We close with a few more general comments. Although we have not yet computed solutions for ρ other than π^{-1} or 1, we believe these $\rho=\pi^{-1}$ results are representative of all incommensurate band fillings. We have also not yet computed results for the next chain length, $N=32$. Attempts to do so indicate that when only 6000 states per iteration are retained, the accumulated errors are too great to allow reliable results to be obtained at this stage of iteration. Finally, this study as a whole suggests that the Hubbard model with only on-site repulsion is inadequate. If U must be as large as our calculation indicates to generate a significant $4k_F$ instability, then for band fillings near half-filled, as is the case for N-methylphenazinium-tetracyanoquinodimethanide (NMP-TCNQ), the large U should cause the $4k_F$ phase to be commensurate[6] and therefore unobservable. Thus the nearest-neighbor Coulomb repulsion (at least) may need to be included also. This we are now doing.

ACKNOWLEDGMENT

One of us (S. T. C.) was supported by the NSF under Grant No. DMR7611338.

[1]S. T. Chui and J. W. Bray, Phys. Rev. B 18, 2426 (1978).
[2]J. Hubbard, Proc. Soc. A 276, 238 (1963); A 281, 401 (1964).
[3]R. E. Peierls, *Quantum Theory of Solids* (Oxford University, London, 1955), p. 108.
[4]J. P. Pouget, S. K. Khanna, F. Denoyer, R. Comes, A. F. Garito, and A. J. Heeger, Phys. Rev. Lett. 35, 445 (1976).
[5]V. J. Emery, Phys. Rev. Lett. 37, 107 (1976).
[6]S. T. Chui and J. W. Bray (unpublished).
[7]J. B. Torrance, Phys. Rev. B 17, 3099 (1978).
[8]E. H. Lieb and F. Y. Wu, Phys. Rev. Lett. 20, 1445 (1968).
[9]H. Fukuyama, T. M. Rice, C. M. Varma, and B. I. Halperin, Phys. Rev. B 5, 3775 (1974); N. Menyhard and J. Solyom, J. Low Temp. Phys. 12, 529 (1973).
[10]C. F. Coll, Phys. Rev. B 9, 2150 (1974).
[11]S. K. Khanna, J. P. Pouget, R. Comes, A. F. Garito, and A. J. Heeger, Phys. Rev. B 16, 1468 (1977).